2020 American Control Conference
Denver, CO, USA, July 1-3, 2020

Power-Preserving Interconnection of Single- and Two-Phase Flow Models for Managed Pressure Drilling*

M.H. Abbasi[1], H. Bansal[1], H. Zwart[2,3], L. Iapichino[1], W.H.A. Schilders[1], N. van de Wouw[2,4]

Abstract— **Many complex systems are modeled by a network of different subsystems, each having their underlying mathematical model representations. Energy-based modeling of each of these subsystems can yield a port-Hamiltonian (pH) representation. In this paper, a single-phase flow model, a dissipative mathematical component and a two-phase flow model are interconnected to model hydraulics for Managed Pressure Drilling (MPD) applications. These subsystems are interconnected in a power-preserving manner to build an aggregated pH system for real-life MPD scenarios. We prove that the interconnection junction connecting the single- and two-phase flow models is conditionally power-preserving.**

I. INTRODUCTION

Port-Hamiltonian (pH) systems have recently received a lot of attention for modeling physical phenomena governed by nonlinear Partial Differential Equations (PDEs) and ordinary differential equations [5], [16]. A pH realization offers a suitable description of the components for the modeling, analysis and controller design [5].

Controllers for PDEs are generally designed for finite-dimensional state-space model descriptions obtained after a low-resolution spatial discretization of the PDEs, which lack part of the information (such as mass conservation) present in the infinite-dimensional representation. Next to PDE control techniques such as optimal control, backstepping [8] and adjoint methods [12], recently, researchers have been investigating control strategies for pH representations [5]. A pH framework enables controller design based on energy consideration by different techniques such as energy-shaping [10], and interconnection and damping assignment [14]. In addition, the Hamiltonian defined in pH framework represents a good candidate for the Lyapunov function, rendering the physics-based control design and the stability proof more tangible [11].

One interesting feature of pH systems is power preservation. A key property of pH systems is that the interconnection of such systems still preserve the pH structure if the interconnection is performed in a power-preserving manner [5], [3]. This compositionality feature enables to interconnect the individual pH subsystems to define an aggregated pH system. A lot of work has already been done in the past in the scope of integration of finite-dimensional and infinite-dimensional components [5], [3]. The key point in aggregating different pH subsystems is the identification of the interconnection structure and casting this interconnection into a power-preserving structure.

Hydraulics in an Managed Pressure Drilling (MPD) can be characterized by interconnection of subsystems governed by a single-phase flow in one pipe and a two-phase flow in another pipe (see Figure 1), and, mathematical models governed by nonlinear ordinary differential equations or static equations [1]. A single-phase flow is usually modelled by the isothermal Euler equations, which obeys a pH formalism [4]. For two-phase flow modelling, the Two-Fluid Model (TFM) and the Drift Flux Model (DFM) are typically employed [1]. Recently, it has been shown that the TFM and a DFM without slippage between the two phases can also be cast in the pH formalism [2]. Drilling with MPD is composed of single- and two-phase flow pH realizations, which can be interconnected via MPD equipment (bit) in a power-preserving manner to form an aggregated pH system.

We employ the existing theory to interconnect (individual) mathematical subsystem models to construct an aggregated model for MPD. To the best of our knowledge, compositional pH modeling for MPD is taken up for the first time in this paper. A compositional pH representation of the MPD model is useful when it needs to be connected to other systems such as a reservoir model, where each system is characterized by a particular energy property. The compositional structure, presented in this work, can be viewed as a stepping stone towards a holistic control paradigm for MPD scenarios. To the best of our knowledge, most controllers for MPD are designed based on a lumped-parameter models approximating the hydraulics and ignoring the fast pressure dynamics [1]. The framework introduced in this paper enables an energy-based controller design while taking all (infinite-dimensional) dynamics into account.

The contribution of this study is two-fold. First, a power-preserving interconnection at the junction connecting the single- and two-phase flow models are provided and, second, a power-preserving condition for a typical junction used in MPD [13] interconnecting these two models is derived. Outside this conditional power-preserving region, the interconnection junction generates power, which renders the

*The first author has carried out this research in the HYDRA project, which has received funding from European Union's Horizon 2020 research and innovation program under grant agreement No 675731. The second author has been funded by the Shell NWO/ FOM PhD Programme in Computational Sciences for Energy Research.

[1]Dept. of Mathematics and Computer Science, Eindhoven University of Technology, The Netherlands, {m.h.abbasi,h.bansal,l.iapichino,w.h.a.schilders}@tue.nl

[2]Dept. of Mechanical Engineering, Eindhoven University of Technology, The Netherlands,n.v.d.wouw@tue.nl

[4]Dept. of Civil, Environmental and Geo-Engineering, University of Minnesota, U.S.A.

[3]Dept. of Applied Mathematics, University of Twente, The Netherlands, h.j.zwart@utwente.nl

junction model (that connects the two subsystems) non-physical.

The structure of this paper is as follows. In Section II, a brief introduction to MPD is provided. In Section III, single- and two-phase flow models together with their pH formalisms are introduced. In Section IV, the interconnection of the single- and two-phase flow models together with the conditional power preservation of the interconnection junction is discussed. In Section V, the power-preserving interconnection of the systems in a real-life drilling scenario is investigated. Finally, Section VI concludes the paper.

II. Managed Pressure Drilling

The industrial problem under investigation is a drilling system, with a special focus on MPD. The configuration of the system is illustrated in Figure 1. A drilling liquid known as mud is pumped into a pipe, called the drillstring, at high pressure. At the bottom of the drillstring, the mud leaves the drillstring through nozzles created inside the drill bit and enters the area between the drillstring and the wellbore, known as the annulus. It then flows up through the annulus and carries the rock cuttings out of the well. In MPD, the annulus is sealed off from the surroundings at the top with a Rotating Control Device (RCD in Figure 1) and the mud circulates out of the well through a choke valve. The circulation path of the mud can be observed by following the green arrows in Figure 1. Usually a flow from the formation containing gas and liquid (this formation is named reservoir in Figure 1) occurs at the bottomhole of the annulus, leading to multi-phase flow in the annulus. For a more comprehensive explanation of MPD, single-phase and two-phase flow modeling, we refer to [13].

Remark 1: If no contingency happens during drilling, the flows inside the drillstring and annulus are of a single-phase flow nature. In case of liquid influx, we assume the reservoir produces the same liquid as the drilling mud. If a gas influx occurs in the formation, the flow inside only the annulus involves two phases.

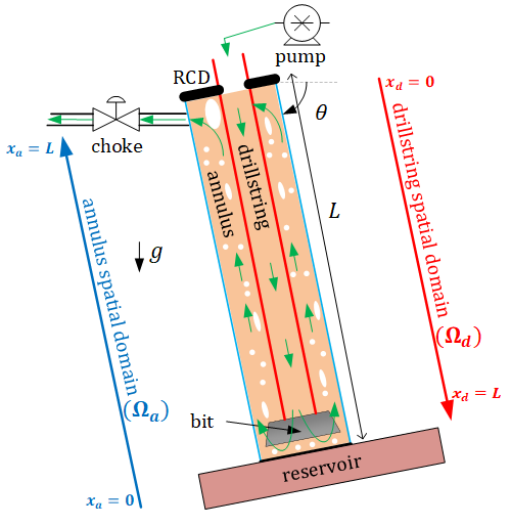

Fig. 1. A drilling well with MPD equipment.

Notation: The following short-hand notations are used in the paper. x_a, x_d: spatial coordinate in the annulus and drillstring, $x_d \in \Omega_d = [0, L]$ and $x_a \in \Omega_a = [0, L]$: spatial domain in the drillstring and annulus, respectively. $(\cdot)^B_{L,d}$: variable $(\cdot)$ at the boundary $x_d = L$, $(\cdot)^{B,i}_{0,a}$: the i-th component of the decomposed variable $(\cdot)$ at the boundary $x_a = 0$, $(\cdot)|_{L,d}$: variable $(\cdot)$ at $x_d = L$, $(\cdot)|^{L,d}_{0,d} := (\cdot)|_{L,d} - (\cdot)|_{0,d}$, $(\cdot)^{B,r,g}_{0,a}, (\cdot)^{B,r,\ell}_{0,a}$: boundary variables at the reservoir for the gas and liquid phase, respectively. Subscripts $(\cdot)_\ell$ and $(\cdot)_g$ refer to the values for liquid and gaseous phase, respectively. $\mathbb{R}$ denotes the space of real numbers.

III. Port-Hamiltonian Models

In this section, we briefly introduce the isothermal Euler equations and the TFM. The pH formulation of each of these models is presented in this section. It should be noted that modeling MPD in 1D captures the most important hydraulics features of drilling [1]. Therefore, the governing PDEs and models for the MPD equipment are presented in 1D.

A. Isothermal Euler Equations

Isothermal Euler equations [9] are typically employed to model single-phase flow inside the drillstring [13]. This model encompasses a coupled mass balance and momentum balance equation. For a drillstring with constant cross-sectional area A_d and a constant inclination of the pipe θ, see Figure 1, under the assumption of laminar flow, the isothermal Euler equations read as follows:

$$\partial_t \rho + \partial_{x_d}(\rho v) = 0, \tag{1a}$$

$$\partial_t(\rho v) + \partial_{x_d}\left(\rho v^2 + p\right) = -32\frac{\mu_\ell v}{d_d^2} + \rho g \sin\theta, \tag{1b}$$

where $t \in \mathbb{R}_{\geq 0}$ and x_d denote the temporal and spatial variables in the drillstring, respectively (see Figure 1). Variables $\rho(t, x_d)$, $v(t, x_d)$ and $p(t, x_d)$ refer to density, velocity and pressure of the mud inside the drillstring, respectively. Moreover, μ_ℓ and d_d denote viscosity of the mud and hydraulic diameter of the drillstring, respectively, and g is the gravitational acceleration. To complete the set of equations, an Equation of State (EOS) is provided as $p = (\rho - \rho_0)c_\ell^2 + p_0$ with constants ρ_0 and p_0 (respectively the density and pressure around which the EOS is linearized), and c_ℓ being the speed of sound in the mud.

The Hamiltonian function for (1) in the state variables $z := [\rho, v]^T$ is

$$\mathcal{H}(z) := A_d \int_{\Omega_d} \rho\frac{v^2}{2} + \rho c_\ell^2 \ln\rho + (c_\ell^2\rho_0 - p_0) - \rho g x \sin\theta \; \mathrm{d}x. \tag{2}$$

In the following theorem, the pH formulation corresponding to (1) is introduced.

Theorem 3.1: The governing equations (1) together with the EOS $p = (\rho - \rho_0)c_\ell^2 + p_0$ can be written in the following dissipative pH formulation:

$$\partial_t z = (\mathcal{J}_d - \mathcal{R}_d(z))\,\delta_z\mathcal{H}(z), \tag{3a}$$

$$\text{with } \mathcal{J}_d = -\frac{1}{A_d}\begin{bmatrix}0 & 1\\ 1 & 0\end{bmatrix}\frac{\partial}{\partial x_d}, \mathcal{R}_d(z) = \begin{bmatrix}0 & 0\\ 0 & \frac{32\mu_\ell}{A_d d_d^2 \rho^2}\end{bmatrix}, \tag{3b}$$

where $z := [\rho,\ v]^T$ and $\mathcal{H}(z)$ is given by (2). This equation is completed by the power conjugated input u and output y at the boundaries with coupling relations as follows:

$$\begin{pmatrix} y^B_{L,d} \\ u^B_{L,d} \end{pmatrix} = \begin{pmatrix} \frac{1}{A_d}\delta_\rho \mathcal{H}(z) \\ \delta_v \mathcal{H}(z) \end{pmatrix} |_{L,d}, \begin{pmatrix} y^B_{0,d} \\ u^B_{0,d} \end{pmatrix} = \begin{pmatrix} -\frac{1}{A_d}\delta_\rho \mathcal{H}(z) \\ \delta_v \mathcal{H}(z) \end{pmatrix} |_{0,d}. \tag{4}$$

Proof: Using (1a) and the EOS, the momentum equation (1b) can be written in terms of ρ and v as

$$\partial_t v = -\partial_{x_d}(\frac{v^2}{2} + c_\ell^2 \ln \rho) - 32\frac{\mu_\ell v}{d_d^2 \rho} + g \sin\theta. \tag{5}$$

The variational derivatives of Hamiltonian (2) are:

$$\delta_\rho \mathcal{H} = A_d(\frac{v^2}{2} + c_\ell^2 \ln \rho + c_\ell^2 - g x_d \sin\theta), \quad \delta_v \mathcal{H} = A_d \rho v. \tag{6}$$

The physical interpretation of $\delta_v \mathcal{H}$ is the mass flow rate of the mud passing spatial location x_d at time t. The energy per unit mass multiplied by the cross section A_d can be inferred from $\delta_\rho \mathcal{H}$. Equations in (3) are obtained by a straightforward replacement of $e_d := [\delta_\rho \mathcal{H},\ \delta_v \mathcal{H}]^T$ in (1a) and (5). Boundary conditions (4) are obtained by satisfying the following relation for the time derivative of the Hamiltonian $\dot{\mathcal{H}}$ and the power through the boundaries of the drillstring $\mathcal{P}^B$,

$$\begin{aligned} &\dot{\mathcal{H}} + \mathcal{P}^B = -\int_{\Omega_d} e_d^T\ \mathcal{R}_d\ e_d\ \mathrm{d}x + \left(\frac{1}{A_d}\delta_\rho \mathcal{H}(z)\delta_v \mathcal{H}(z)\right)|_{0,d} - \\ &\left(\frac{1}{A_d}\delta_\rho \mathcal{H}(z)\delta_v \mathcal{H}(z)\right)|_{L,d} + y^B_{0,d}u^B_{0,d} + y^B_{L,d}u^B_{L,d} = \\ &-\int_{\Omega_d} e_d^T\ \mathcal{R}_d\ e_d\ \mathrm{d}x \le 0. \end{aligned} \tag{7}$$

The last inequality is due to the positive semi-definite nature of $\mathcal{R}_d(z)$. ∎

B. Two-Fluid Model

The TFM can be defined in terms of PDEs expressing mass and momentum conservation laws for each phase in the annulus with constant cross-sectional area A_a, constant hydraulic diameter d_a and constant inclination θ as follows [15]:

$$\partial_t(\alpha_i \rho_i) + \partial_{x_a}(\alpha_i \rho_i v_i) = 0, \tag{8a}$$

$$\begin{aligned} \partial_t(\alpha_i \rho_i v_i) + \partial_{x_a}(\alpha_i \rho_i v_i^2) = -\partial_x(\alpha_i p_a) + \\ M_i - \alpha_i \rho_i g \sin\theta - 32\frac{\mu_g \alpha_i v_i}{d_a^2}, \end{aligned} \tag{8b}$$

where $i \in \{\ell, g\}$ and x_a is the spatial variable in the annulus (see Figure 1). The model contains seven unknown variables, namely, liquid and gas void fraction, α_ℓ and α_g, liquid and gas phase velocity, v_ℓ and v_g, liquid and gas phase density, ρ_ℓ and ρ_g, and the common pressure in the annulus p_a. To complete the model, we use a set of widely applied closure laws as in [6]:

$$\alpha_g + \alpha_\ell = 1, \tag{9a}$$

$$M_g + M_\ell = 0, M_g = p_a \partial_x \alpha_g + b_g^M(v_\ell - v_g), \tag{9b}$$

$$\rho_g = \frac{p_a}{c_g^2}, \rho_\ell = \rho_0 + \frac{p_a - p_0}{c_\ell^2}, \tag{9c}$$

where (9a) expresses that any pipe segment is occupied by the combination of gas and liquid. The terms M_g and M_ℓ with the constant $b_g^M \ge 0$ in (9b) account for the force interaction between the phases. Finally, (9c) define the barotropic EOS of each phase with c_g the constant speed of sound in the gaseous phase.

The Hamiltonian for the flow inside the annulus with $z_a := [m_g,\ m_\ell,\ v_g,\ v_\ell]^T$ takes the following form (with $m_g := \alpha_g \rho_g$ and $m_\ell := \alpha_\ell \rho_\ell$):

$$\begin{aligned} \mathcal{H}_a(z_a) := A_a \int_{\Omega_a} m_g \frac{v_g^2}{2} + m_\ell \frac{v_\ell^2}{2} + m_g c_g^2 \ln \rho_g + m_\ell c_\ell^2 \ln \rho_\ell + \\ \alpha_\ell(c_\ell^2 \rho_0 - p_0) - (m_\ell + m_g)\, g(L - x) \sin\theta\ \mathrm{d}x. \end{aligned} \tag{10}$$

Notably, variables $\rho_\ell, \rho_g, \alpha_\ell$ can be written in terms of m_g and m_ℓ, see [2]. In the following theorem, the pH formulation corresponding to (8) and (9) is presented.

Theorem 3.2: The governing equations (8) associated with the closure equations (9) can be written in the dissipative pH formulation as follows:

$$\partial_t z_a = (\mathcal{J}_a - \mathcal{R}_a(z_a))\, \delta_{z_a} \mathcal{H}_a(z_a), \tag{11a}$$

$$\mathcal{J}_a = -\frac{1}{A_a}\begin{bmatrix} \mathbf{0} & \mathrm{I} \\ \mathrm{I} & \mathbf{0} \end{bmatrix} \frac{\partial}{\partial x_a}, \mathcal{R}_a(z_a) = \frac{1}{A_a}\begin{bmatrix} \mathbf{0} & \mathbf{0} \\ \mathbf{0} & \tau \end{bmatrix}, \tag{11b}$$

where $z_a := [m_g,\ m_\ell,\ v_g,\ v_\ell]^T$ and $\mathcal{H}_a$ is given by (10), $\tau = \begin{bmatrix} \frac{b_g^M}{m_g^2} + \frac{32\mu_g\alpha_g}{m_g^2 d^2} & -\frac{b_g^M}{m_g m_\ell} \\ -\frac{b_g^M}{m_g m_\ell} & \frac{b_g^M}{m_\ell^2} + \frac{32\mu_l\alpha_\ell}{m_\ell^2 d^2} \end{bmatrix}$, and $\mathbf{0}$ and I denote the 2×2 zero and identity matrix, respectively. This pH formulation is completed by the power conjugated inputs u and outputs y at the boundary coupled with relations as follows:

$$\begin{pmatrix} y^{B,1}_{0,a} \\ y^{B,2}_{0,a} \\ u^{B,1}_{0,a} \\ u^{B,2}_{0,a} \end{pmatrix} = \begin{pmatrix} -\frac{1}{A_a}\delta_{m_g}\mathcal{H}_a \\ -\frac{1}{A_a}\delta_{m_\ell}\mathcal{H}_a \\ \delta_{v_g}\mathcal{H}_a \\ \delta_{v_\ell}\mathcal{H}_a \end{pmatrix} |_{0,a}, \begin{pmatrix} y^{B,1}_{L,a} \\ y^{B,2}_{L,a} \\ u^{B,1}_{L,a} \\ u^{B,2}_{L,a} \end{pmatrix} = \begin{pmatrix} \frac{1}{A_a}\delta_{m_g}\mathcal{H}_a \\ \frac{1}{A_a}\delta_{m_\ell}\mathcal{H}_a \\ \delta_{v_g}\mathcal{H}_a \\ \delta_{v_\ell}\mathcal{H}_a \end{pmatrix} |_{L,a}. \tag{12}$$

Proof: Rewriting momentum equations (8b) in terms of v_g and v_ℓ leads to

$$\begin{aligned} \partial_t v_i + \partial_{x_a}\left(\frac{v_i^2}{2}\right) = -c_i^2 \partial_{x_a}(\ln \rho_i) \pm \frac{b_g^M}{m_i}(v_\ell - v_g) \\ - g \sin\theta - 32\frac{\mu_i v_i}{\rho_i d_a^2}, \end{aligned} \tag{13}$$

where "+" is used for $i = g$ and "−" is used for $i = \ell$. Using the Hamiltonian (10) (for details, see [2]),

$$\begin{cases} \delta_{m_i}\mathcal{H}_a = A_a(\frac{v_i^2}{2} + c_i^2 \ln \rho_i + c_i^2 - g(L - x_a)\sin\theta), \\ \delta_{v_i}\mathcal{H}_a = A_a m_i v_i, \quad i \in \{\ell, g\}. \end{cases} \tag{14}$$

Similar to the isothermal Euler equations, $\delta_{v_i}\mathcal{H}_a$ represents the mass flow rate of the phase i. Similarly, The energy per unit mass of phase i multiplied by the cross section A_a can be inferred from $\delta_{m_i}\mathcal{H}_a$. Straightforward replacement of these relations into the original equations give the asserted equations. Similar to Theorem 3.1, the boundary terms can be obtained from ($\mathcal{P}_a^B$ is the power through the boundaries

of annulus)

$$\dot{\mathcal{H}}_a + \mathcal{P}_a^B = -\int_{\Omega_a} e_a^T\ \mathcal{R}_a\ e_a\ \mathrm{d}x + \left(\frac{1}{A_a}\delta_{m_g}\mathcal{H}_a\delta_{v_g}\mathcal{H}_a\right)|_{0,a} + \left(\frac{1}{A_a}\delta_{m_\ell}\mathcal{H}_a\delta_{v_\ell}\mathcal{H}_a\right)|_{0,a} - \left(\frac{1}{A_a}\delta_{m_g}\mathcal{H}_a\delta_{v_g}\mathcal{H}_a\right)|_{L,a} - \left(\frac{1}{A_a}\delta_{m_\ell}\mathcal{H}_a\delta_{v_\ell}\mathcal{H}_a\right)|_{L,a} + y_{0,a}^{B,1}u_{0,a}^{B,1} + y_{0,a}^{B,2}u_{0,a}^{B,2} + y_{L,a}^{B,1}u_{L,a}^{B,1} + y_{L,a}^{B,2}u_{L,a}^{B,2} = -\int_{\Omega_a} e_a^T\ \mathcal{R}_a\ e_a\ \mathrm{d}x \leq 0,$$

with $e_a = [\delta_{m_g}\mathcal{H}_a, \delta_{m_\ell}\mathcal{H}_a, \delta_{v_g}\mathcal{H}_a, \delta_{v_\ell}\mathcal{H}_a]^T$. ■

Remark 2: PH properties for the isothermal Euler equations in [4] and the TFM in [2] are proved for only unit cross section without frictional and gravitational source terms. Moreover, a different choice of the state variables than in [2] is employed to express the pH realization of the TFM.

Remark 3: It can easily be proved that $\mathcal{J}_d$ in (3) and $\mathcal{J}_a$ in (11) are formally skew-adjoint operators [5]. Moreover, $\mathcal{R}_d$ and $\mathcal{R}_a$ in the same equations are symmetric positive semi-definite.

IV. Power-Preserving Interconnection

In this section, the drillstring, the drill bit and the annulus are connected in a power-preserving manner. First, the boundary conditions are introduced. Then, the dissipation of energy through the bit is studied. Finally, the power-preserving structure of the interconnection junction (the bit and the summation junction at the reservoir, see Figure 2) is investigated.

A. Boundary conditions of the single- and two-phase flow models in MPD

The boundary conditions governing the fluid flow in the drillstring and the annulus follow from Figure 1. The governing equations of the pump, bit and choke are summarized in Table I. For the pump, $\dot{m}_p, A_p, \rho_p$ and v_p represent the mass flow rate, the cross-sectional area, the density and the velocity of the liquid through the pump, respectively. For the bit, $\Delta p_b, \rho_b, \dot{m}_b, A_N$ and C_D denote the pressure drop over the bit, density at the drillstring side of the bit, the mass flow rate through the bit, the total area of the nozzles of the bit and the nozzle coefficient, respectively. For the choke, $\dot{m}_c, \rho_c, p_c$ and p_0 are the mass flow rate, the density, the pressure at the choke inlet and atmospheric pressure, respectively. Finally, K_c and z_c, are the choke constant and the choke opening, respectively.

First, we define the boundary conditions for the drillstring to be used in (4).

TABLE I

Governing equations of the pump, bit and choke.

Equipment	Governing equation
pump	$\dot{m}_p = A_p\rho_p v_p$
bit	$\Delta p_b = \frac{1}{2\rho_b}\left(\frac{\dot{m}_b}{A_N C_D}\right)^2$
Choke	$\dot{m}_c = K_c z_c\sqrt{2\rho_c\,(p_c - p_0)}$

Pump: At the pump location, we have $A_p = A_d, v_p = v|_{0,d}$ and $\rho_p = \rho|_{0,d}$. Hence

$$\delta_v\mathcal{H}|_{0,d} = (\rho A_d v)|_{0,d} = \dot{m}_p(t). \tag{15}$$

The boundary condition at the left side of the spatial domain Ω_d is assigned. Input and output variables at this boundary can be defined with (15) and (4).

Bit and reservoir: Through the bit, the mass conservation holds and the pressure drop is governed by the bit equation. Moreover, the flow that passed through the bit is then mixed with the known liquid mass flow rate $\dot{m}_\ell(t)$ and the gaseous mass flow rate $\dot{m}_g(t)$ coming out of the reservoir. Then, the mixture enters the annulus. Considering $\Delta p_b = p|_{L,d} - p|_{0,a}, \dot{m}_b = (\rho A_d v)|_{L,d}, \rho_b = \rho|_{L,d}$, we have

$$\begin{cases} p|_{L,d} - p|_{0,a} = \dfrac{1}{2\rho|_{L,d}}\left(\dfrac{\delta_v\mathcal{H}|_{L,d}}{A_N C_D}\right)^2, \\ \delta_v\mathcal{H}|_{L,d} + \dot{m}_\ell(t) = \delta_{v_\ell}\mathcal{H}_a|_{0,a}, \\ \delta_{v_g}\mathcal{H}_a|_{0,a} = \dot{m}_g(t). \end{cases} \tag{16}$$

Remark 4: To solve the TFM, typically either 2 boundary conditions are specified at the left side of the domain and 2 at the right side or 3 boundary conditions at the left side and one at the right [7]. In this paper, we consider the 2-2 case. In (16), one equation corresponds to the right boundary for the isothermal Euler equations in the drillstring and two equations correspond to the left boundary of the TFM in the annulus.

Remark 5: Above the bit and inside the drillstring, a non-return valve is installed to restrict the flow in one direction only from the drillstring to the annulus. When this valve is open, the pressure drop over the bit is governed by the bit equation in Table I. When this valve is closed, the drillstring and the annulus become disconnected. Then, the right boundary condition for the drillstring becomes $\dot{m}_b(t) = (\rho A_d v)|_{L,d} = 0$ and therefore $\delta_v\mathcal{H}|_{L,d} = 0$. The left boundary condition for the annulus changes to $\delta_{v_\ell}\mathcal{H}_a|_{0,a} = \dot{m}_\ell(t)$ and $\delta_{v_g}\mathcal{H}_a|_{0,a} = \dot{m}_g(t)$.

Choke: For the TFM at the choke, we have two boundary conditions, i.e., the explicit value of gas void fraction over time and the nonlinear choke equation. Following the same procedure in [13], we rewrite $\dot{m}_c$ as the mass flow rate of the mixture, $\dot{m}_c = (\rho_\ell A_a v_\ell)|_{L,a} + (\rho_g A_a v_g)|_{L,a}$. We also replace ρ_c with the mixture density, $\rho_c = \alpha_\ell\rho_\ell + \alpha_g\rho_g$. Therefore, we have:

$$\begin{aligned} (\delta_{v_\ell}\mathcal{H}_a + \delta_{v_g}\mathcal{H}_a)|_{L,a} &= K_c z_c\sqrt{2(m_g + m_\ell)|_{L,a}\,(p_a|_{L,a} - p_0)}, \\ \alpha_g|_{L,a} &= g(t), \end{aligned} \tag{17}$$

where $g(t)$ is a function of time, explicitly specifying the gas void fraction at the choke.

Remark 6: Notably, boundary conditions (16) and (17) form an implicit function of variational derivative of Hamiltonian (2) and (10) with respect to z and z_a, respectively.

Remark 7: For the case of 2-2 boundary conditions specified above, setting the boundary inputs to zero leads to $\dot{\mathcal{H}}_a = 0$ in the absence of dissipation. For the case of 3-1 boundary conditions, setting the boundary inputs to zero will not yield the same result and it is not clear how energy of the system evolves over time. This complicates the energy perspective presented in this paper for 3-1 case.

B. Dissipativity of power through the bit

The power-preserving structure of the single-phase flow model and the TFM are shown in Section III by the corresponding dissipative pH formulation of (3)-(4) and (11)-(12).

In this section, we derive conditions under which the interconnections, shown in Figure 2, are power-preserving. To have power-preserving interconnections, we define the following interconnections between input ports u and output ports y of different components shown in Figure 2:

$$\begin{cases} u_{d,bit} = y^{B}_{L,d} \\ y_{d,bit} = -u^{B}_{L,d} \end{cases}, \begin{cases} u_{a,bit} = y_1 \\ y_{a,bit} = -u_1 \end{cases}, \begin{cases} u_2 = y^{B,2}_{0,a} \\ y_2 = -u^{B,2}_{0,a} \end{cases}, \\ \begin{cases} u_3 = y^{B,r,\ell}_{0,a} \\ y_3 = -u^{B,r,\ell}_{0,a} \end{cases}, \begin{cases} u^{B,r,g}_{0,a} = y^{B,1}_{0,a} \\ y^{B,r,g}_{0,a} = -u^{B,1}_{0,a} \end{cases}. \tag{18}$$

The power preservation of all these connections can be easily checked [5], e.g., $u_2 y_2 + u^{B,2}_{0,a} y^{B,2}_{0,a} = 0$. If the power is preserved through the bit, then the entire aggregated system preserves power. Therefore, we only focus on deriving the condition of power preservation through the bit.

Remark 8: Due to the directions shown in Figure 1, the positive direction is assumed from pump to the bit and from the bit to the choke. Therefore, the incoming power into bit flows from the drillstring and the outgoing power from the bit enters the annulus.

The physical nature of the bit dictates the outgoing power to be less than the incoming power (see Figure 2)

$$\mathcal{P}_{bit} := u_{a,bit} y_{a,bit} - u_{d,bit} y_{d,bit} \leq 0. \tag{19}$$

The incoming power $u_{d,bit} y_{d,bit}$ is related to the physical variables of the system via (18). To relate the outgoing power $u_{a,bit} y_{a,bit}$ to the model-dependent variables, the power preservation across the summation junction is written as

$$\begin{aligned} &u_1 y_1 + u_2 y_2 + u_3 y_3 = 0 \xrightarrow{(18)} \\ &(-u_{a,bit} y_{a,bit}) + (-u^{B,2}_{0,a} y^{B,2}_{0,a}) + (-u^{B,r,\ell}_{0,a} y^{B,r,\ell}_{0,a}) = 0, \end{aligned} \tag{20}$$

where $u^{B,\mathrm{r},\ell}_{0,a} := -\dot{m}_\ell(t)$ and, by considering the definition of the boundary conditions in the pH formulations (4) and (12), we have $u^{B,2}_{0,a} = \dot{m}_b + \dot{m}_\ell(t)$ and $y^{B,2}_{0,a} = -\frac{1}{A_a}\delta_{m_\ell}\mathcal{H}_a|_{0,a}$. For the summation junction, we use a 1-junction principle where all outputs are equal and the summation of all inputs equal to zero. This leads to $y^{B,\mathrm{r},\ell}_{0,a} = -\frac{1}{A_a}\delta_{m_\ell}\mathcal{H}_a|_{0,a}$, Then by using (16) in (20), we obtain,

$$u_{a,bit} y_{a,bit} = \frac{1}{A_a}\dot{m}_b \ \delta_{m_\ell}\mathcal{H}_a|_{0,a}. \tag{21}$$

Substituting (21), (16) into (19) yields

$$\mathcal{P}_{bit} = \dot{m}_b \left(\frac{1}{A_a}\delta_{m_\ell}\mathcal{H}_a|_{0,a} - \frac{1}{A_d}\delta_\rho \mathcal{H}|_{L,d} \right). \tag{22}$$

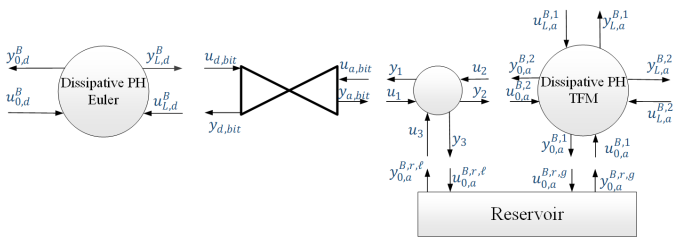

Fig. 2. The power-preserving interconnection of different components of a drilling well.

Note that when the non-return valve is closed, the two systems become isolated and the summation of the power change of both is less than the summation of the input-output conjugated energy of each pipe. As the non-return valve is open, $\dot{m}_b > 0$ holds. To ensure the power-preserving property across the bit, we must ensure $\mathcal{P}_{bit} \leq 0$. As a result of this property and by using (22), we have

$$\frac{1}{A_d}\delta_\rho \mathcal{H}|_{L,d} - \frac{1}{A_a}\delta_{m_\ell}\mathcal{H}_a|_{0,a} \geq 0. \tag{23}$$

Replacing the terms describing the variational derivative of Hamiltonian with respect to state variables from (6) and (14) leads to

$$\begin{aligned} &(\frac{v^2}{2} + c_\ell^2 \ln\rho - gL\sin\theta)|_{L,d} - \\ &(\frac{v_\ell^2}{2} + c_\ell^2 \ln\rho_\ell - gL\sin\theta)|_{0,a} \geq 0 \rightarrow \\ &\frac{1}{2}M_d^2(-\frac{M_a^2}{M_d^2} + 1) + \ln\frac{\rho|_{L,d}}{\rho_\ell|_{0,a}} \geq 0, \end{aligned} \tag{24}$$

where $M_d = \frac{v|_{L,d}}{c_\ell}, M_a = \frac{v_\ell|_{0,a}}{c_\ell}$ are the Mach numbers of the flow at the outlet of the drillstring and at the inlet of the annulus near the bit. To further simplify the relation, we use the bit equation,

$$\Delta p_b = (\rho|_{L,d} - \rho_\ell|_{0,a})c_\ell^2 = \frac{1}{2}\rho|_{L,d}(\frac{A_d}{A_N C_D})^2 v|^2_{L,d} \rightarrow \tag{25a}$$

$$\frac{\rho_\ell|_{0,a}}{\rho|_{L,d}} = 1 - \frac{1}{2}(\frac{A_d}{A_N C_D})^2 M_d^2, \tag{25b}$$

The mass conservation across the bit (16) can also be simplified to

$$\begin{aligned} &(A_d\rho v)|_{L,d} + \dot{m}_\ell(t) = (A_a\rho_\ell v_\ell)|_{0,a} \rightarrow A_d M_d + \frac{\dot{m}_\ell(t)}{\rho c_\ell} = \\ &A_a\frac{\rho_\ell}{\rho}M_a \xrightarrow{(25)} M_a = \frac{A_d}{A_a}\frac{M_d}{1 - \frac{1}{2}(\frac{A_d}{A_N C_D})^2 M_d^2} + M_{\ell_r}, \end{aligned} \tag{26}$$

where $M_{\ell_r} := \frac{\dot{m}_\ell(t)}{A_a c_\ell \rho_\ell|_{0,a}}$ is the Mach number at the interface of the reservoir and annulus. Finally by using (26), the inequality (24) simplifies to

$$\begin{aligned} \mathcal{M} :=& \frac{1}{2}M_d^2((\frac{A_d}{A_a}\frac{1}{1 - \frac{1}{2}(\frac{A_d}{A_N C_D})^2 M_d^2} + \frac{M_{\ell_r}}{M_d})^2 - 1) \\ &+ \ln(1 - \frac{1}{2}(\frac{A_d}{A_N C_D})^2 M_d^2) \leq 0. \end{aligned} \tag{27}$$

For the bit, connecting the drillstring and the annulus, to be power-preserving, the inequality (27) should hold.

V. Numerical example

In this section, a real drilling well is considered and the region where the inequality (27) holds is investigated. The corresponding geometry and bit property are studied to define the power-preserving operational region. Outside this region, the bit model should be adjusted to abide power preservation.

Remark 9: In drilling operations, the velocity inside the drillstring is typically around 1 m/s while the speed of sound in the mud is around 1000 m/s. Therefore, for drilling applications, $M_d \approx 0.001$.

The geometry and equipment properties of the drilling platform are given by

$$\begin{aligned} &d_d = 76.2 \text{ mm}, d_{od} = 241.3 \text{ mm}, d_w = 444.5 \text{ mm}, \\ &A_N = 1418.7 \text{ mm}^2, C_D = 0.8, \end{aligned} \tag{28}$$

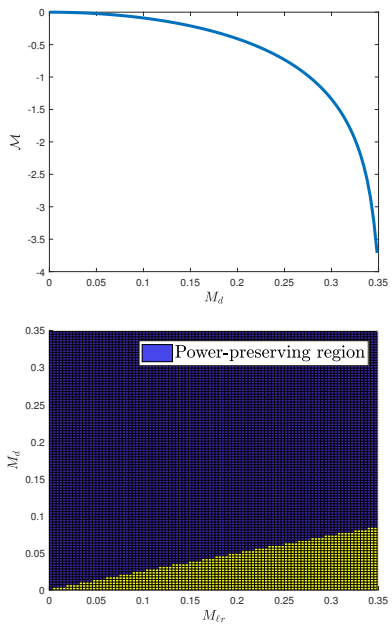

Fig. 3. Top: The value of the function $\mathcal{M}$ in (27) for different admissible Mach number with $\dot{m}_\ell = 0$, Below: Power-preserving region for different Mach numbers of M_d and M_{ℓ_r} satisfying inequality (27).

where d_{od} and d_w are, respectively, the outer diameter of the drillstring and the diameter of the wellbore.

For this well and this drill bit, to render the argument inside the logarithmic function in (27) to be positive, we observe that $M_d < 0.35$ should hold. As shown in the top part of Figure 3, in this restricted region for M_d with no flow from the reservoir (which is true in the normal drilling scenarios), (27) always holds for $\dot{m}_\ell = 0$ for the drilling well under consideration and the bit model is indeed dissipative (power-preserving). This might be the experimental condition under which the model for the bit was derived.

In case of contingencies, where the fluid of the reservoir flows into the annulus, condition (27) is not always satisfied in the restricted region for M_d, as shown in the bottom part of Figure 3. When the reservoir also contains liquid, the velocity of this flow should be less than the velocity of the flow coming through the bit. This situation most probably occurs when the drilling process and the mud injection are halted ($M_d = 0$) and a new pipe section is added to the drillstring to increase its length to drill further (this is called a *connection* scenario in practice). If the reservoir is producing liquid during connection, this inequality does not hold for sure. Therefore, the bit model presented in Table I must not be used to simulate the hydraulics in this situation. Notably, in cases when velocity of the flow from the reservoir is much higher than the velocity of the flow passing through the bit, usually the non-return valve is closed and the two subsystems become isolated. This situation, however, requires more investigation. These bit models are usually derived by curve fitting to experimental data obtained under certain conditions. To adapt the bit model, experiments should be designed in such a way that the inequality (27) is violated and a new model should be fitted to the new data.

VI. Conclusion

In this paper, two pH models for the (single- and two-phase) flow dynamics in MPD with nonlinear boundary conditions are interconnected by a nonlinear drill bit model. To render the aggregated system power-preserving, the mathematical model of the bit, used to interconnect the two pipes, obeys power preservation under a certain condition. However, this conditional power preservation does not restrict the normal drilling operation region. The drill bit model restricts the drilling operation where liquid influx from reservoir flows into the wellbore. In such cases, velocity of the drilling mud at the bit inside the annulus should be higher than the velocity of the liquid influx. Outside this region, the power preservation of the bit model might be violated. The framework proposed in this paper enables an energy-based controller design for MPD while taking the infinite-dimensional nature of the dynamics into account.

References

[1] U. Aarsnes. *Modeling of two-phase flow for estimation and control of drilling operations*. PhD thesis, NTNU, 2016.

[2] H. Bansal, M. Abbasi, P. Schulze, H. Zwart, L. Iapichino, W. Schilders, and N. van de Wouw. Port-Hamiltonian formulation of two-phase flow models. Available online at `https://www.win.tue.nl/~hbansal/draft-version-to-be-submitted.pdf`, 2020.

[3] J. Cervera, A. van der Schaft, and A. Banos. Interconnection of port-Hamiltonian systems and composition of dirac structures. *Automatica*, 43(2):212–225, 2007.

[4] H. de Wilde. *Port-Hamiltonian discretization of gas pipeline networks*. MSc. Thesis Applied Mathematics, Groningen University, 2015.

[5] V. Duindam, A. Macchelli, S. Stramigioli, and H. Bruyninckx. *Modeling and control of complex physical systems: the port-Hamiltonian approach*. Springer, 2009.

[6] S. Evje and T. Flatten. On the wave structure of two-phase flow models. *SIAM Journal of Applied Mathematics*, 67(2):487–511, 2007.

[7] A. Figueiredo, R. Baptista, F. de Freitas Rachid, and G. Bodstein. Numerical simulation of stratified-pattern two-phase flow in gas pipelines using a two-fluid model. *International Journal of Multiphase Flow*, 88:30–49, 2017.

[8] M. Krstic and A. Smyshlyaev. *Boundary control of PDEs: a course on backstepping designs*. Philadelphia, PA: Society for Industrial and Applied Mathematics, 2008.

[9] R. LeVeque. *Finite Volume Methods for Hyperbolic Problems*. Cambridge University Press, 2002.

[10] A. Macchelli, Y. L. Gorrec, and H. Ramirez. Boundary energy-shaping control of an ideal compressible isentropic fluid in 1-d. *IFAC-PapersOnLine*, 50(1):5598–5603, 2017.

[11] A. Macchelli and C. Melchiorri. Modeling and control of the timoshenko beam. the distributed port Hamiltonian approach. *SIAM Journal on Control and Optimization*, 43(2):743–767, 2004.

[12] C. Meyer, R. Arnd, and T. Fredi. Optimal control of pdes with regularized pointwise state constraints. *Computational Optimization and Applications*, 33(2-3):209–228, 2006.

[13] S. Naderi Lordejani, M. H. Abbasi, N. Velmurugan, C. Berg, J. A. Stakvik, B. Besselink, L. Iapichino, F. Di Meglio, W. H. A. Schilders, and N. van de Wouw. Modeling and numerical implementation of managed pressure drilling systems for evaluating pressure control systems. *In press SPE Drilling & Completion*, 2020.

[14] R. Ortega, A. van der Schaft, B. Maschke, and G. Escobar. Interconnection and damping assignment passivity-based control of port-controlled hamilonian systems. *Automatica*, 38:585–596, 2002.

[15] I. Tiselj and S. Petelin. Second order numerical method for two-fluid model of air-water flow. *Nuclear Society of Slovenia*, 1995.

[16] A. van der Schaft and D. Jeltsema. Port-Hamiltonian systems theory: An introductory overview. *Foundations and Trends in Systems and Control*, 1(2):173–378, 2014.